frontiers | Frontiers in Materials

TYPE Original Research
PUBLISHED 09 November 2023
DOI 10.3389/fmats.2023.1277247

OPEN ACCESS

EDITED BY
Suresh Sagadevan,
University of Malaya, Malaysia

REVIEWED BY
Ravi Kumar Cheedarala,
Changwon National University, Republic of Korea
Kartik Nemani,
Purdue University, United States

*CORRESPONDENCE
Shucai Zhang,
zhangsc.qday@sinopec.com

RECEIVED 14 August 2023
ACCEPTED 30 October 2023
PUBLISHED 09 November 2023

CITATION
Wang W, Song X, Xie Y, Sheng X and Zhang S (2023), A study on the preparation of superhydrophobic Silane-MXene modified melamine foam and its oil-water separation performance. *Front. Mater.* 10:1277247. doi: 10.3389/fmats.2023.1277247

A study on the preparation of superhydrophobic Silane-MXene modified melamine foam and its oil-water separation performance

Wei Wang, Xiangning Song, Yan Xie, Xuejia Sheng and Shucai Zhang*

State Key Laboratory of Chemical Safety, SINOPEC Research Institute of Safety Engineering Co, Ltd., Qingdao, China

In recent years, oil spills and organic pollution have caused severe damage to the ecological environment. Therefore, the treatment of oily wastewater has become a serious challenge. Here, with the help of melamine foams as a substrate, MXene nano-rough structures were built, and cetyltrimethoxysilane was grafted onto their surfaces to create an oil-absorbing material that is both user-friendly and effective at oil-water separation. Due to the nano structures of MXene were constructed and the long-chain silanes were modified on the foam surface, the material became superhydrophobic. In addition to being able to selectively absorb oils from an oil/water mixture (including emulsified oils) up to 111 times its weight, the modified foam was found to have a water contact angle of 157 which could selectively absorb oil but not water. Furthermore, it demonstrated sustained hydrophobicity and lipophilicity after experiencing strong acid/alkali or prolonged high-temperature treatment, allowing for various scenarios where oil-water separation can be used in severe settings without compromising performance.

KEYWORDS

melamine foam, oil-water separation, MXene, long-chain silane, superhydrophobic

1 Introduction

Despite the petrochemical industry's meteoric rise in recent decades, oil and organic waste streams from oil extraction, transportation, and chemical accidents pose serious threats to ecosystems and human health (Shannon et al., 2008; Dalton and Jin, 2010). As a result, there is a pressing need to develop low-cost and effective technologies for extracting oil and organic solvents from oily effluent. To date, techniques such as physical adsorption, chemical redox, and microbiological degradation have been developed to lessen the ecological harms caused by oily effluent (Beshkar et al., 2017; Lv et al., 2017; Doshi et al., 2018; Peng et al., 2018) Physical adsorption has emerged as a promising approach and research focus for oil leakage disposal and recycling because of its simple operation, low environmental impact, high efficiency, and absence of secondary contamination compared to chemical redox and microbiological degradation, respectively (Zhang et al., 2021). Hence, many different types of porous and high-specific surface-area materials, such as wool fibres, cotton, activated carbon, straw, and polymer foams, are utilized for physical adsorption. Melamine foam (MF), a polymer with a three-dimensional mesh structure, is a suitable substrate for adsorbent materials (Nguyen et al., 2012; Pham and Dickerson, 2014; Zhu et al., 2015) due to its high porosity, outstanding mechanical capacity, wide availability of sources,

and low cost. However, water and oil are frequently co-adsorbed on the surfaces of the aforementioned porous materials, which have poor oil-water selectivity, making hydrophobic alteration of the surfaces of the porous materials necessary to achieve the desired wettability (Zhang et al., 2016a).

To create ultra-light, flame-retardant, compressible, superhydrophobic adsorbent materials, Yang et al. (Yang et al., 2014) started with melamine-formaldehyde foam and modified it hydrophobically with silane. Chitosan foams were modified by Duan et al. (Duan et al., 2014) by adding acetamides via freeze-drying, followed by chemical vapour deposition to create a methyltrichlorosilane coating, which produced oil-absorbent foams with interconnected open pore architecture, high toughness, and mechanical strength. In recent years, new methods (Jayaramulu et al., 2016; Li et al., 2018) for oil-water separation have emerged with the advent of two-dimensional (2D) materials. Superhydrophobic rGO/polyurethane foams were made by Xia et al. (Xia et al., 2018) using the solvothermal method in an ethanol environment. These foams have water contact angles of up to 153° and can adsorb oils at a rate of more than 37 times their weights. Chen et al. (Chen et al., 2019) coated foams with octadecylamine-grafted rGO, which enabled the foam to absorb 44–111 times its weight in oil. Utilizing an ultrasonic technique, Krasian et al. (Krasian et al., 2019) were able to develop MoS_2-WS_2/polylactic acid polymer with excellent oil adsorption and oil-water separation capabilities by hybridizing the 2D materials MoS_2 and WS_2.

Naguib et al. (Naguib et al., 2011) made the initial discovery of MXene, a brand-new 2D transition metal carbide and nitride, in 2011. One of the most researched and anticipated 2D materials now available, MXene has a layered structure, diverse interfacial chemistry, and outstanding mechanical properties (Shahzad et al., 2016; Yan et al., 2017; Gogotsi and Anasori, 2019; Lin et al., 2020). $M_{n+1}X_nT_x$ (n = 1, 2, 3) is the general formula for MXene, where M denotes a transition metal element, X for a C or N element, and T_x denotes a surface functional group like = O, -OH, -F, etc., (Zhao et al., 2018; Wang et al., 2019; Song et al., 2021). MXene offers a sizable contact area and a changeable surface chemical structure due to its high specific surface area and the profusion of reactive groups on its surface (Saththasivam et al., 2019; Feng et al., 2020). An efficient approach was reported by Liu et al. (Liu et al., 2017) to fabricate freestanding, flexible, and hydrophobic MXene foam with reasonable strength by assembling MXene sheets into films followed by a hydrazine-induced foaming process. Wu et al. (Wu et al., 2023) fabricated silane modified MXene/polybenzazole nanocomposite aerogels with exceptional surface hydrophobicity, flame retardance and thermal insulation by using a combined sol-gel, freeze-dry and thermal treatment approach.

In the present study, the surface of commercial melamine foam (MF) was covered with MXene 2D nanostructures in order to improve the roughness of the MF. In a subsequent process, hydrophobic long-chain silanes were further grafted onto the functional groups on MXene to create a new adsorbent material that can effectively separate oil from water in real-world complex oil-bearing wastewater systems.

2 Materials and methods

2.1 Materials and apparatus

Commercial melamine foam (MF), purchased from Sichuan Chaoju New Materials Technology Co., Ltd.; MXene ($Ti_3C_2T_x$) aqueous dispersion, purchased from Jiangsu XFNANO Materials Tech Co., Ltd.; cetyltrimethoxysilane, Sudan III, methylene blue, Tween-80, purchased from Shanghai Macklin Biochemical Co., Ltd.; ethanol, methylene chloride, soybean oil, purchased from Shanghai Aladdin Biochemical Technology Co., Ltd.; lubricant, purchased from Hasitai Lubricant Co., Ltd. Shanghai; 0# diesel, purchased from Sinopec Gas Station.

Fourier transform infrared spectrometer (FTIR, Nicolet, United States, model Nicolet 5,700); scanning electron microscope-X-ray energy dispersive spectrometer (SEM-EDS, Hitachi, Japan, model SU3800); X-ray photoelectron spectrometer (XPS, Thermo Fisher, UK, model ESCALAB 250Xi); contact angle meter (JEOL, Japan, model JC 2000D2); electronic universal testing machine (MTS Systems (China) Co., Ltd., model CMT 2503).

2.2 Preparation of superhydrophobic melamine foam

First, the commercial melamine foam (MF) was cut into 1 × 1 × 1 cm^3 cubes and ultrasonically washed for 3 h with deionized water and ethanol. The washed MF foams were placed in a blast dryer and dried for 10 h at 80°C. Following that, the aqueous MXene dispersion was configured with a concentration of 0.02–0.1 mg/mL, and so on. After being cleansed, MF foams were submerged in MXene dispersion of varying concentrations, gently compressed, and soaked to fill the MF foam's interior with MXene dispersion, then removed and freeze-dried overnight. MXene@MF was the label assigned to the samples. Then, a solution of cetyltrimethoxysilane/ethanol (at a concentration of 0.05–0.15 mg/mL) was prepared. The MXene@MF foam was immersed in different concentrations of cetyltrimethoxysilane/ethanol solution ranging from 0.05–0.15 mg/mL, slightly squeezed to ensure that it was entirely filled, removed, and vacuum dried at −0.1 MPa and 80°C for 10 h. Finally, the sample was washed 3 times with ethanol to eliminate any remaining siloxane on the surface before being vacuum dried again for 10 h. The superhydrophobic melamine foam samples were successfully obtained and labelled as Silane-MXene@MF.

2.3 Characterization

The structural characterization of melamine-modified foam in the wave number range of 500–4,000 cm^{-1} was carried out using a Fourier transform infrared spectroscopy (FTIR, Nicolet, the United States, model Nicolet 5,700) in total reflection mode; the surface morphology of melamine-modified foam was examined using a scanning electron microscope-X-ray energy dispersive spectrometer (SEM-EDS, Hitachi, Japan, model SU3800); the elemental analysis of melamine-modified foams was performed using an X-ray photoelectron spectrometer (XPS, Thermo Fisher Scientific, the UK, model ESCALAB 250Xi); the hydrophobicity of the foam was tested using a contact angle meter (JEOL, Japan, model JC 2000D2) by adding 4 μL of water dropwise to the foam surface and recording the water contact angle (WCA) and taking the average of five tests at different random locations on the surface and its profile; the cyclic compression performance of the foam was tested using an electronic universal testing machine (CMT 2503, MTS

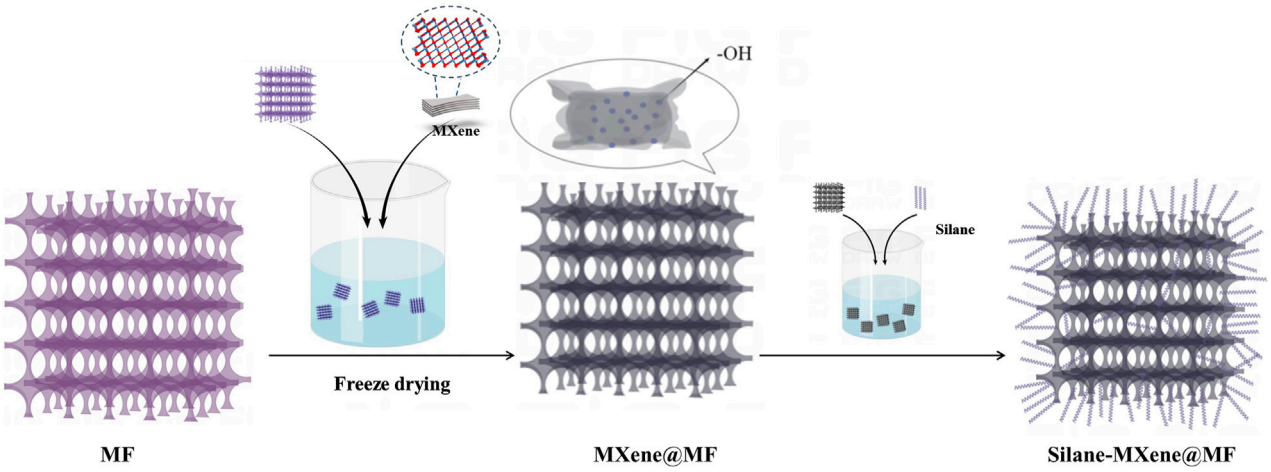

FIGURE 1
Schematic diagram of the preparation of Silane-MXene@MF.

Systems (China) Co., Ltd.) at a compression rate of 10 mm/min at room temperature. The oil absorption rate test was conducted to characterize the oil absorption properties of the superhydrophobic melamine foam using soybean oil, lubricating oil, 0# diesel oil, toluene, and methylene chloride, respectively. The following equation was used to compute the oil absorption rate K:

$$K = \frac{m_2 - m_1}{m_1} \quad (1)$$

where m_1 is the net foam mass, and m_2 is the mass of the foam after oil absorption. For the separation efficiency test, a highly emulsified oil/water mixture was prepared by placing 1 mL of 0# diesel oil with 50 mg of Tween-80 into 100 mL of water; the mixture was magnetically stirred for 2 h to ensure complete emulsification of the diesel oil in the water; the foam was placed in a syringe to separate the oil/water mixture, and the permeate flux F was calculated as follows: (Liu and Yuan, 2018)

$$F = V/(S \cdot t) \quad (2)$$

where V is the volume of the mixture (L), S is the effective area of the filter material (m^2) and t is the separation time (h). The separation efficiency R is calculated as follows: (Chen et al., 2016)

$$R = \left(1 - C_f/C_0\right) \times 100\% \quad (3)$$

where C_f and C_0 represent the volume fraction of oil (vol%) in the filtrate and feed, respectively, and the volume fraction of oil in water was measured by an infrared spectrophotometer (Tianjin Tianguang Optical Instrument Co., Ltd., model TJ270-30A).

3 Results and discussion

3.1 Preparation of Silane-MXene@MF

Figure 1 illustrates the synthesis of Silane-MXene@MF. After freeze-drying, MXene nanosheets were attached to the surface of MF foam by electrostatic forces and intermolecular interaction forces, which could considerably increase the surface roughness of MF. The MXene surface of MXene@MF, on the other hand, was abundant in hydroxyl groups and could be employed as a secondary reaction platform for the subsequent reaction stage. MXene@MF was next immersed in a highly hydrolysable cetyltrimethoxysilane/ethanol solution, and the resulting hydrolysis products were silylated with the hydroxyl group on the surface of MXene in order to graft long-chain silanes onto the MXene@MF surface to reduce the surface free energy of the materials (Qian et al., 2020). In this step, the hydroxyl group was reacted off, so the hydrophilicity of MXene was greatly reduced. The synergistic effect of the nano-rough surface structure of Silane-MXene@MF and the low surface free energy of the long-chain silanes conferred superhydrophobicity on Silane-MXene@MF. Physical pictures of samples with varying MXene and silane contents are shown in Figure 2. Figures 2A–C are Silane-MXene@MF samples with concentrations of 0.02 mg/mL MXene and concentrations of 0.05, 0.1, and 0.15 mg/mL silane; Figures 2D–F are Silane-MXene@MF samples with concentrations of 0.06 mg/mL MXene and concentrations of 0.05, 0.1, and 0.15 mg/mL silane, and Figures 2G–I are Silane-MXene@MF samples with concentrations of 0.1 mg/mL MXene and concentrations of 0.05, 0.1, and 0.15 mg/mL silane, respectively. As the MXene concentration increases, it can be noticed that the colour of Silane-MXene@MF darkens, further demonstrating MXene's increased adhesion to the foam skeleton's surface.

3.2 Structural characterization of Silane-MXene@MF

Fourier transform infrared spectroscopy (FTIR) was employed for the structural analysis of the foam samples. The infrared spectra of MF, MXene, MXene@MF, and Silane-MXene@MF are displayed in Figure 3A. The IR absorption peaks at 3,340 cm^{-1} are the N-H stretching vibrations in the MF foam, while the IR absorption peaks at 1,557, 1,328, and 810 cm^{-1} are the C=N stretching vibrations, C-N stretching vibrations, and triazine ring stretching vibrations in the

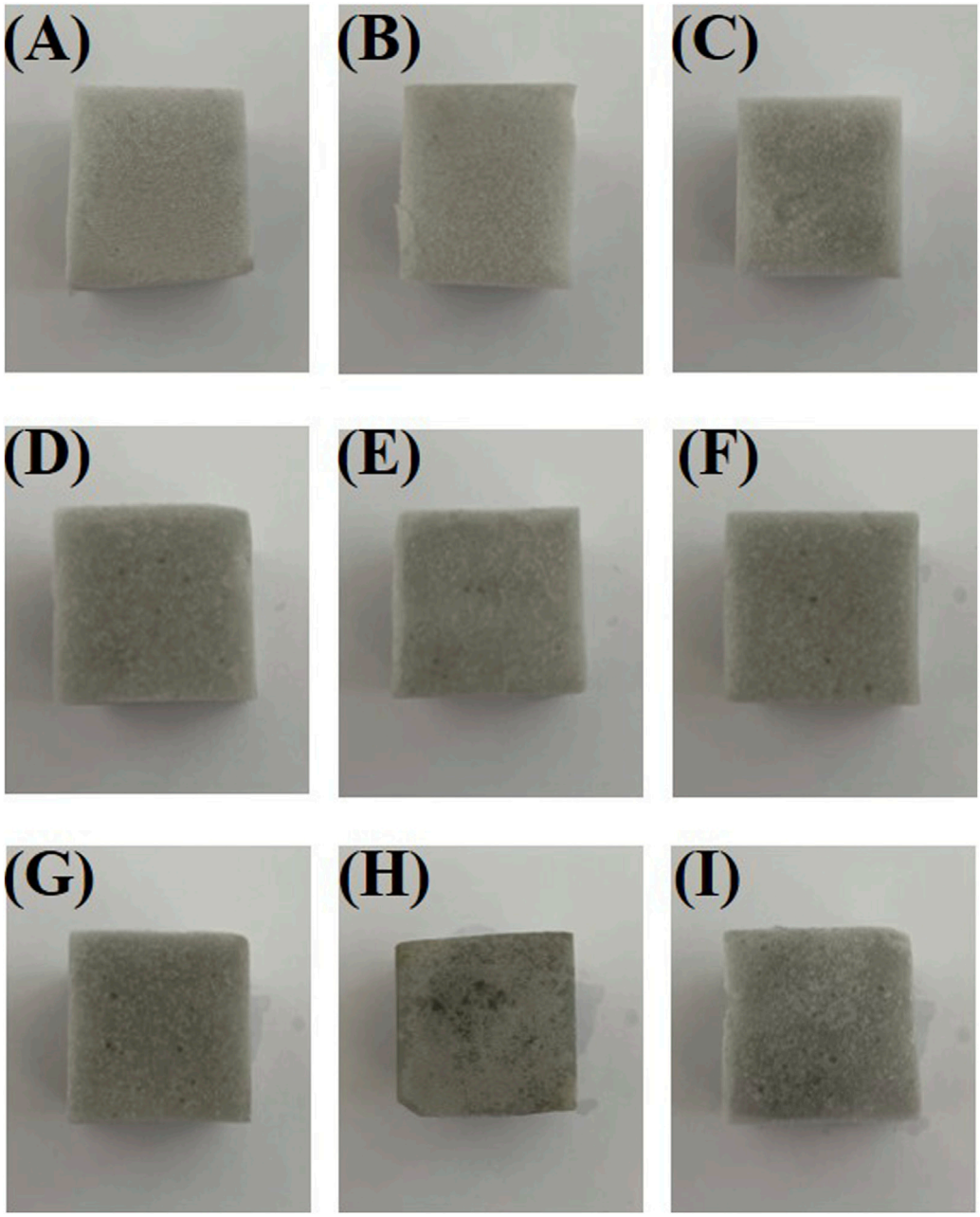

FIGURE 2
Physical picture of samples of different formulations of Silane-MXene@MF. Silane-MXene@MF samples with concentrations of 0.02 mg/mL MXene and concentrations of 0.05, 0.1, and 0.15 mg/mL silane **(A–C)**; concentrations of 0.06 mg/mL MXene and concentrations of 0.05, 0.1, and 0.15 mg/mL silane **(D–F)**; concentrations of 0.1 mg/mL MXene and concentrations of 0.05, 0.1, and 0.15 mg/mL silane **(G–I)**.

triazine ring of the MF foam, respectively (Zhang et al., 2016b). Regarding MXene, the IR absorption peaks at 580, 1,617, and 3,267 cm^{-1} correspond to the stretching vibrations of Ti-O, -C=O, and -OH, respectively (Xue et al., 2021). After freeze-drying, the MXene nanosheets were adhered to the MF foam surface by electrostatic forces and intermolecular interactions, and the IR spectra of MXene@MF revealed the characteristic absorption peaks of MF and MXene with no additional absorption peaks being produced. Cetyltrimethoxysiloxane was grafted onto the foam skeleton surface in Silane-MXene@MF as a result of the MXene nanosheets' plentiful -OH. After siloxane hydrolysis, the antisymmetric stretching vibration of Si-O-Si resulted in the IR absorption peak at 1,089 cm^{-1}. This suggested that the skeleton of the melamine foam has been modified by siloxane and MXene nanosheets.

X-ray photoelectron spectroscopy (XPS) was applied to more thoroughly characterize the elemental composition and structure of MF and the modified Silane-MXene@MF. The results are displayed in Figure 3B. MF possesses only C, N and O elements. The Silane-MXene@MF sample exhibited a notable increase in the intensity of the

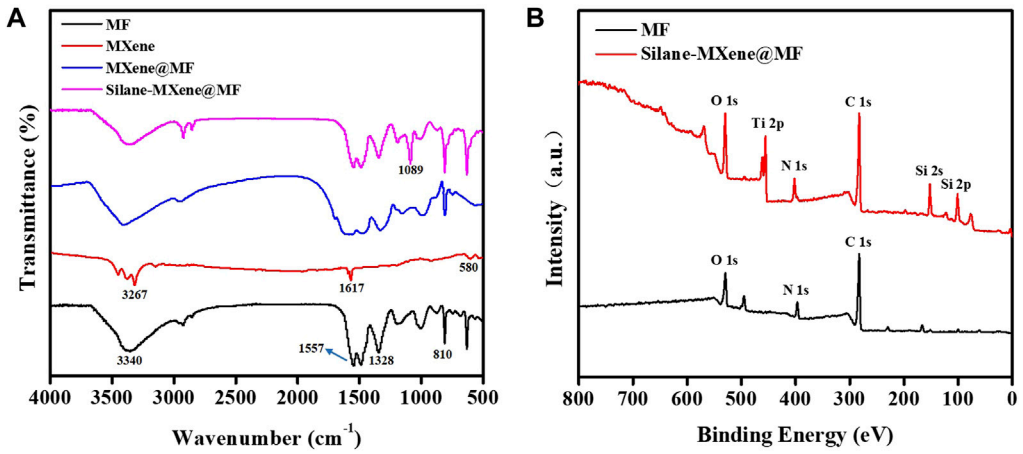

FIGURE 3
Infrared spectrogram of MF, MXene, MXene@MF and Silane-MXene@MF **(A)**; XPS energy spectra of MF and Silane-MXene@MF **(B)**.

Ti 2p peak when compared to MF. Obviously, Ti was introduced by MXene, providing more evidence for the effective attachment of MXene to the MF surface (Wang et al., 2019). Additionally, the XPS energy spectrum of Silane-MXene@MF revealed Si 2p and Si 2s peaks, proving the successful grafting of cetyltrimethoxysilane onto the MXene@MF surface. Actually, the cetyltrimethoxysilane hydrolysate is silanized with the hydroxyl group on the surface of MXene, resulting in the grafting of long-chain silanes onto the foam surface (Qian et al., 2020). In conclusion, the XPS findings further showed that MXene was smoothly modified with cetyltrimethoxysilane on the surface of MF, which was compatible with the FTIR results.

3.3 Analysis of surface topography

Using scanning electron microscopy (SEM), the surface morphology of MF was examined in order to clarify the impact of MXene and long-chain silane. Figures 4A–F displays SEM pictures of MF and Silane-MXene@MF. As shown in Figures 4A–C, both a complete 3D porous network structure and a smooth surface structure may be seen in the pristine melamine foam (Zhang et al., 2016b), which diameter was a few microns, and the pore diameter of the pristine melamine foam ranges from tens to hundreds of microns. The microscopic morphology of the modified Silane-MXene@MF foam is depicted in Figures 4D–F. The attachment of MXene and long-chain silanes to the surface of the Silane-MXene@MF foam skeleton resulted in a rough surface. This is due to the fact that the MXene nanosheets were modified on the MF surface through electrostatic and intermolecular interaction forces, which increases the surface roughness through stacking effect. It can be seen in Figure 4F, the MXene on the foam skeleton of the Silane-MXene@MF are wrinkled, which can improve the wettability. Although MXene covered the pore structure of melamine sponge to a certain extent, it did not obstruct the open channel of foam, these indicated that Silane-MXene@MF completely inherited the microporous structure of melamine foam in the coating process. X-ray energy dispersive spectroscopy (EDS) was used to further analyze the Silane-MXene@MF's elemental composition, as shown in Figure 4G. According to the EDS spectrum, Silane-MXene@MF is mostly composed of the elements C, N, O, Si and Ti, with Si standing for cetyltrimethoxysilane and Ti for MXene. Such elements were evenly dispersed throughout the foam, and the foam skeleton structure can be displayed, indicating that MXene and long-chain silane were uniformly bonded to the surface of the MF skeleton.

3.4 Analysis of surface wettability

Surface wettability is essential to the design of oil-water separation materials. The wettability of Silane-MXene@MF is primarily expressed as the contact angle with water or oil. As can be seen in Figure 5A, water was stained blue by methylene blue, and diesel oil was stained red by Sudan III. When drops of water and oil were placed on the surface of virgin foam MF, both water and oil were promptly absorbed, proving that the contact angle of oil and water was almost 0°. In contrast, the modified Silane-MXene@MF speedily adsorbed oil, and the oil droplets were completely immersed in the surface, indicating that its oil contact angle was nearly 0°, whereas the water droplets were spherical on the surface of Silane-MXene@MF, as shown in Figure 5B, and the water contact angle could reach up to 157.4°. This means that Silane-MXene@MF is extremely hydrophobic and lipophilic, capable of selectively absorbing oil but not water. When Silane-MXene@MF was placed in water, as shown in Figure 5C, the foam floated on the surface without becoming wet. Additionally, the silver mirror phenomenon occurred at the foam-water interface, which was heavily covered in tiny bubbles (Wang and Lin, 2013), demonstrating Silane-MXene@MF's excellent water repellency. This difference in wettability before and after modification is due to the fact that the original MF foam surface is smooth and contains a large number of hydrophilic functional groups, which are hydrophilic and oleophilic, whereas the foam modified by MXene and long-chain silane has a surface with a nano-rough structure and hydrophobic chain segments with a low surface energy that trap tiny air bubbles on its surface and thereby prevent water intrusion.

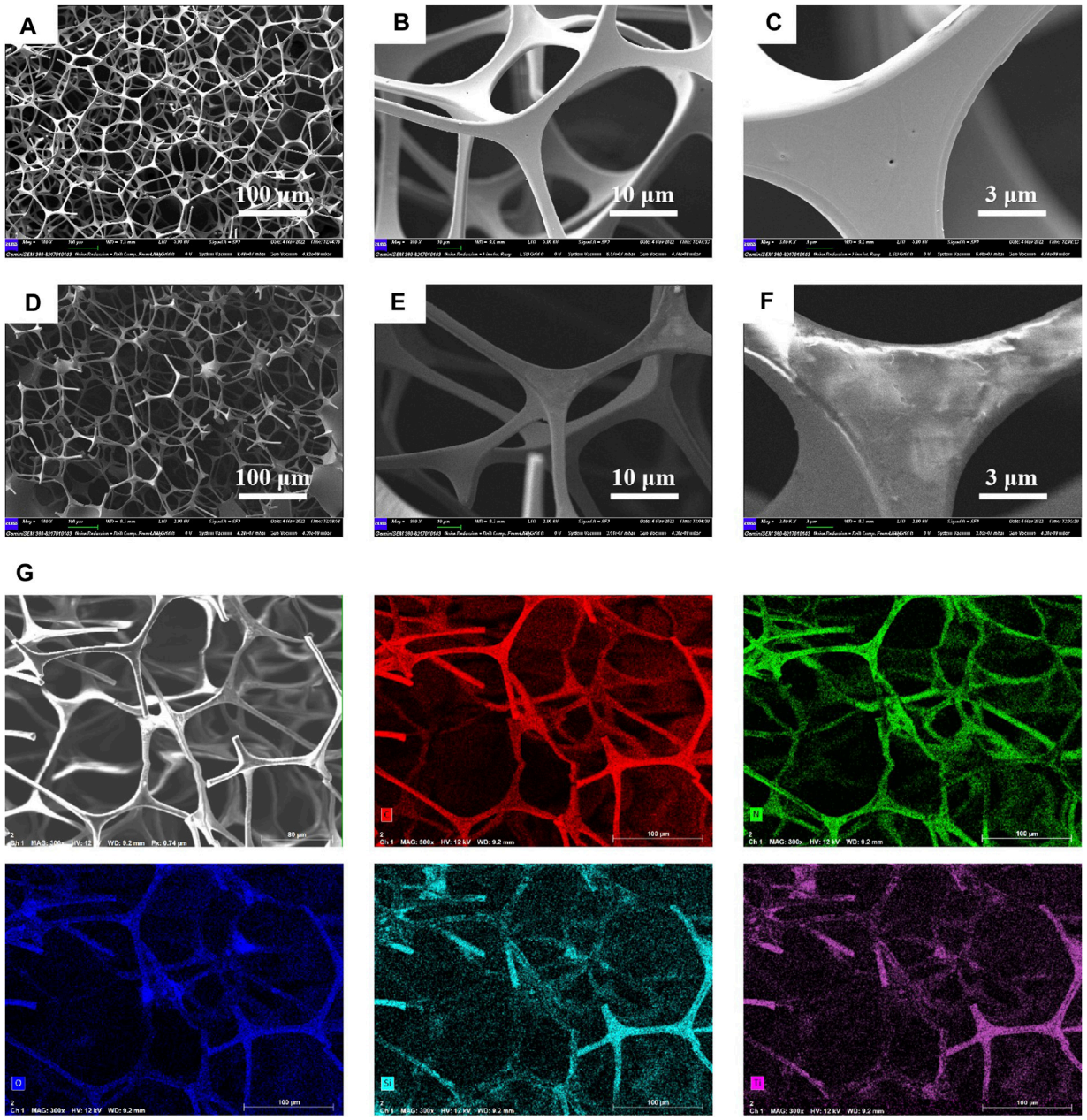

FIGURE 4
SEM Graph of MF **(A–C)** and Silane-MXene@MF **(D–F)**; X-ray energy dispersion spectrum of Silane-MXene@MF **(G)**.

Figure 5D illustrates the effect of MXene and silane concentrations on the water contact angle (WCA) of Silane-MXene@MF, whereas Figures 5E–G depicts the contact angle of Silane-MXene@MF with MXene and silane concentrations of 0.02, 0.05 mg/mL; 0.1, 0.05 mg/mL; 0.1, 0.15 mg/mL, from left to right. It is evident that the WCA rises as MXene and silane concentrations rise, demonstrating that MXene and silane have a substantial effect on the surface wettability of the foam. The presence of more nano-rough surfaces on a material's surface means that more tiny bubbles can be retained on the water's surface, increasing the material's ability to separate water and resulting in superhydrophobicity. Long-chain silane can reduce the foam's surface free energy and increase its hydrophobicity. This low surface free energy and surface roughness have a synergistic impact that turns the MF foam from hydrophilic and lipophilic to superhydrophobic and superlipophilic.

3.5 Analysis of oil absorption capacity

The nano-rough surface, low surface free energy, and three-dimensional porosity of Silane-MXene@MF make it very superhydrophobic and superoleophilic with a high oil storage capacity. Due to its capillary forces and super-oleophilicity, Silane-MXene@MF can rapidly absorb oil and organic debris

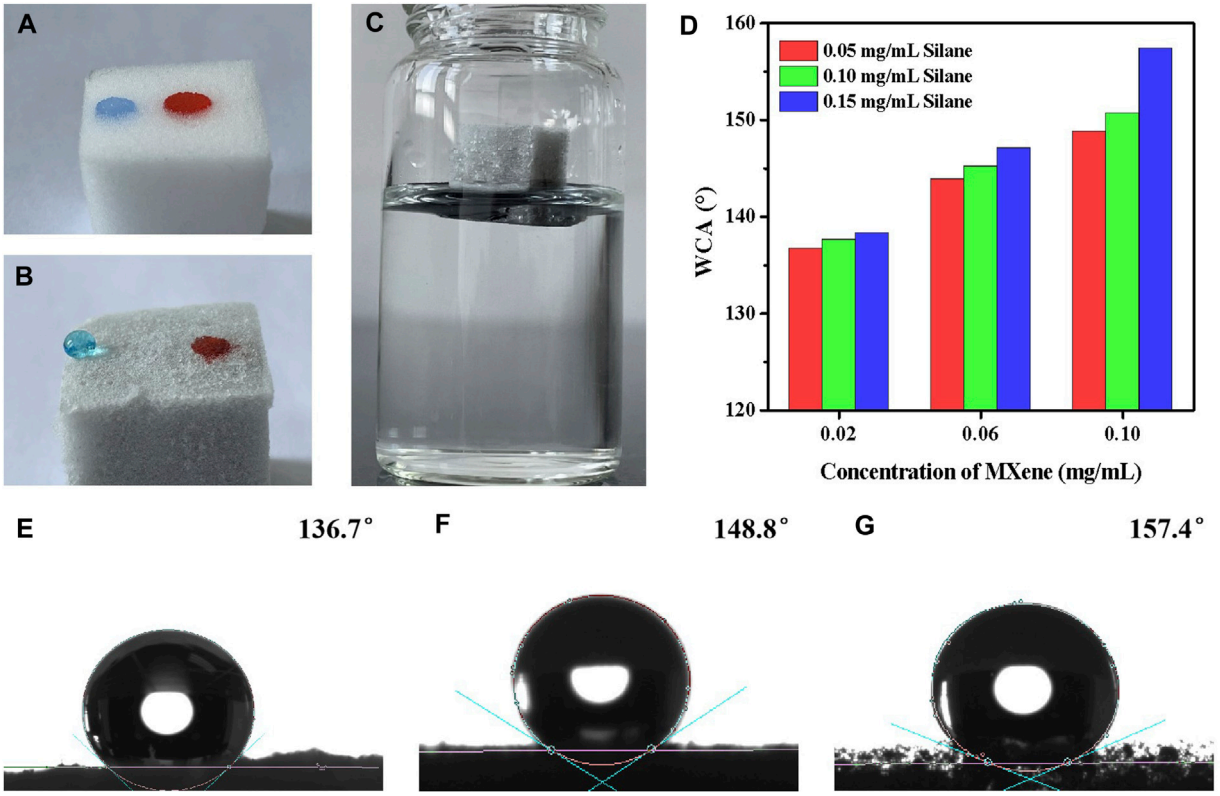

FIGURE 5
Physical picture of water droplets (stained by methylene blue) and oil droplets (stained by Sudan III) on the surface of MF **(A)** and Silane-MXene@MF **(B)**; **(C)** Silane-MXene@MF in water; **(D)** Effect of MXene and silane concentration on the water contact angle (WCA) of Silane-MXene@MF; **(E–G)** Picture of the contact angle of Silane-MXene@MF (MXene and silane concentrations from left to right: 0.02, 0.05 mg/mL; 0.1, 0.05 mg/mL; 0.1, 0.15 mg/mL).

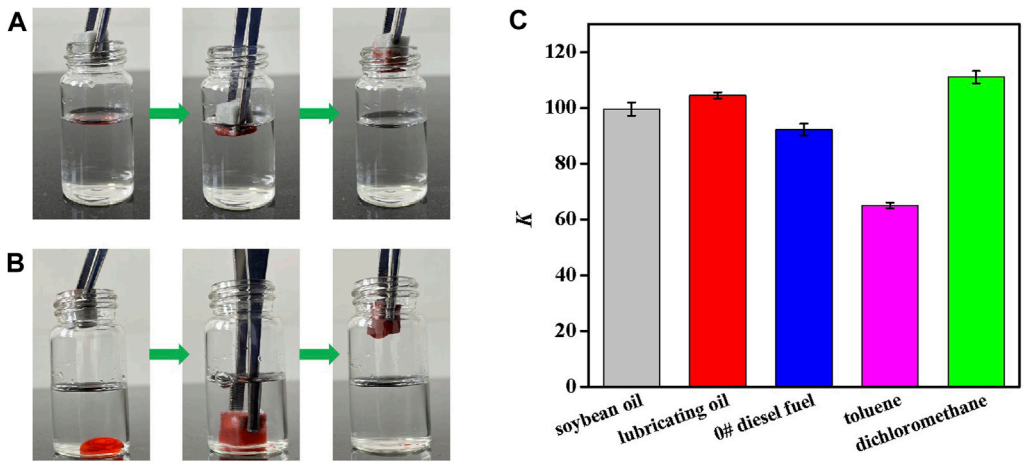

FIGURE 6
Photographs of the absorption process of Silane-MXene@MF on diesel (stained by Sudan III)/water mixture **(A)** and dichloromethane (stained by Sudan III)/water mixture **(B)**; **(C)** Oil absorption rate *K* of Silane-MXene@MF on different oils and organics.

from the oil/water mixture upon contact. Sudan III was employed to stain 0# diesel and methylene chloride as surface-floating and subsurface-sinking oil contaminants. Figure 6A showed how Silane-MXene@MF immediately and completely absorbed oil from the diesel/water mixture when it was placed on the diesel/water mixture, achieving rapid oil-water separation on the water surface. As seen in Figure 6B, as Silane-MXene@MF was submerged in a dichloromethane/water mixture and exposed

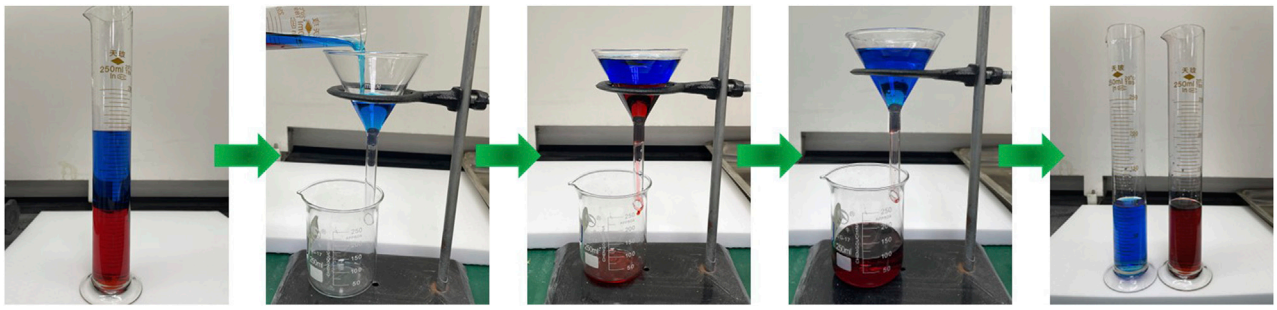

FIGURE 7
Separation process of oil/water mixture.

to the dichloromethane, the organic solvent was quickly absorbed. Actually, Silane-MXene@MF can absorb a wide variety of oil and organic matters, whether they are on the water's surface or below it, without absorbing water in the process, and the adsorbed oils/organic solvents could be recoverable through manual squeezing. The oil absorption rate *K* of Silane-MXene@MF for various oils and organics is listed in Figure 6C. The modified foam exhibits a high absorption capacity for oils and organic solvents with values of 99.6, 104.5, 92.2, 65.0, and 111.0 for soybean oil, lubricating oil, 0# diesel, toluene, and methylene chloride, respectively, ranging up to 111 times its weight because of the different density of the oil/organic solvents and the limited volume of foam. This indicates that Silane-MXene@MF has excellent absorption performance in different oil/water mixtures.

3.6 Analysis of oil-water separation capacity

As can be seen in Figure 7, the oil-water separation performance of Silane-MXene@MF was tested by filtering the oil/water mixture through an adsorption foam. A mixture of methylene chloride and water was prepared, with the methylene chloride stained by Sudan III and the water stained by methylene blue. Methylene chloride was placed at the bottom of the mixture due to the fact that it is denser than water. The dichloromethane/water mixture was progressively poured into the funnel after Silane-MXene@MF was plugged into the funnel hole. Initially, water was poured into the funnel, but it did not drip, showing that Silane-MXene@MF had greater water resistance. As dichloromethane entered the funnel, it was preferentially absorbed by Silane-MXene@MF. After saturation, a channel was created. Gravity caused dichloromethane to pass through the foam and fall into the beaker beneath. After the dichloromethane evaporated, water continued to build above the funnel, demonstrating that Silane-MXene@MF is superhydrophobic and lipophilic, enabling the efficient separation of oil/water mixtures. The oil-water separation of emulsified oil/water mixture has been a pressing challenge, so the efficacy of Silane-MXene@MF for the oil-water separation of emulsified oil/water mixture was investigated further. 100 mL of water was combined with 1 mL of 0# diesel fuel and 50 mg of Tween-80, and the mixture was magnetically swished for 2 h to create the oil/watere mulsion. As depicted in Figure 8, the emulsified oil/water mixture was filtered by pouring it into a syringe containing Silane-MXene@MF. The oil/water mixture was gravity-fed through Silane-MXene@MF,

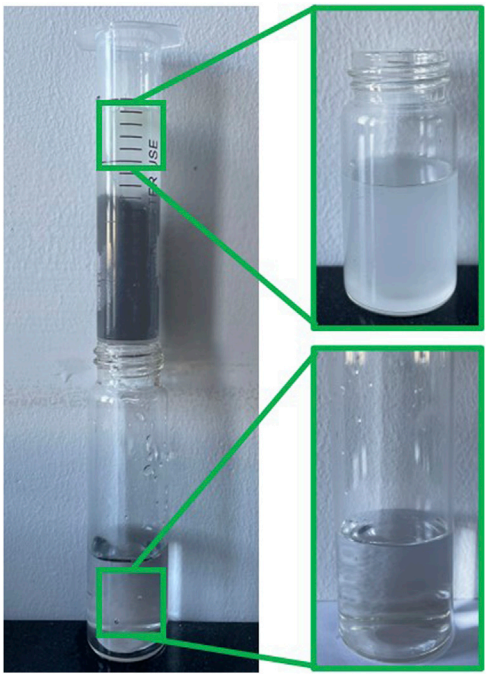

FIGURE 8
Separation process of emulsified oil/water mixture.

resulting in a clean filtrate. The permeate flux *F* for the diesel/water emulsion was up to 1354 L $m^{-2}{\cdot}h^{-1}$ and the separation efficiency was as high as 93.12%. The nano-rough structure of Silane-MXene@MF comes into contact with the tiny oil droplets when the emulsified oil/water mixture strikes the foam's inner wall. This causes the oil droplets to gradually gather on the surface of the nanostructure while the water molecules pass through the pores, resulting in the separation of emulsified oil from oil/water mixture.

3.7 Mechanical and chemical stability

Mechanical capacity and stability are two of the most difficult challenges constraining the use of oil-water separation materials; hence, it is essential that Silane-MXene@MF has a high mechanical

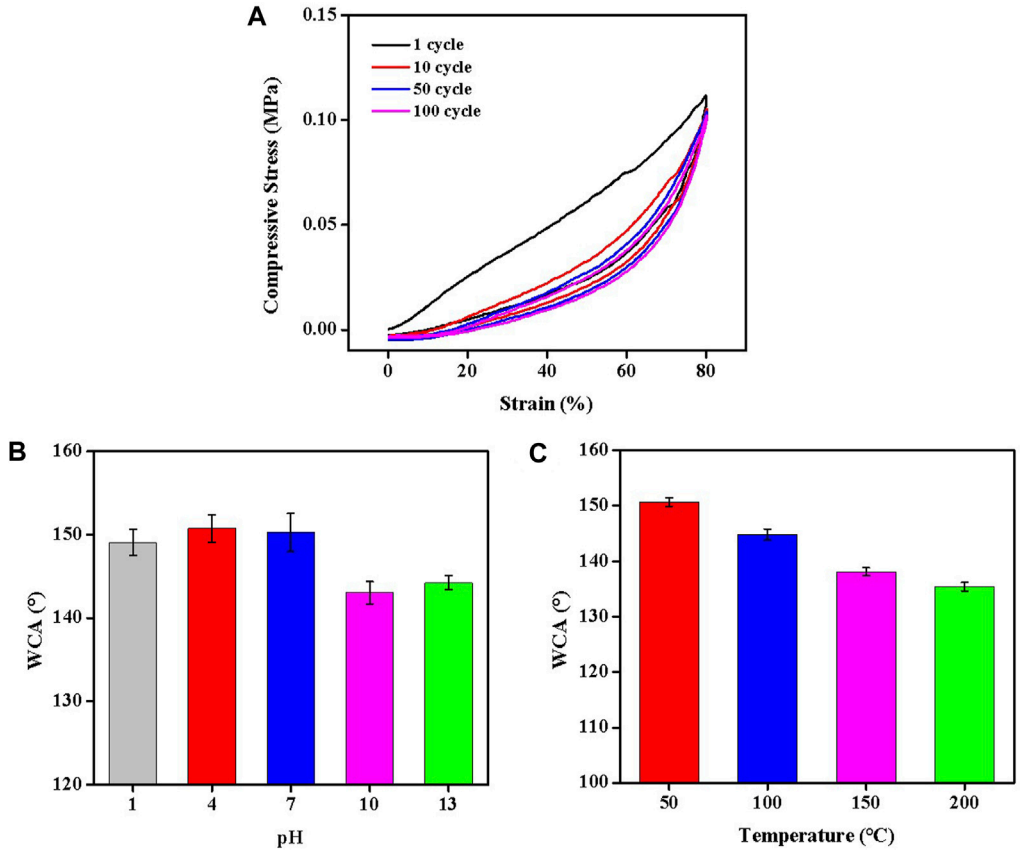

FIGURE 9
(A) 100 cycles of compression experiments at 80% strain; water contact angle (WCA) of Silane-MXene@MF at different pH **(B)** and temperature **(C)**.

capacity and stability for a wide range of real-world applications under harsh conditions. As a result, the cyclic compression performance of Silane-MXene@MF was examined, as illustrated in Figure 9A. The nonlinearity and closed hysteresis of the Silane-MXene@MF's stress-strain curve reveal the typical high deformability of such materials (Xu et al., 2010). The foam may almost completely recover its original shape after being compressed and released 1, 10, 50, and 100 times at 80% strain. After 100 compression cycles, the maximum stress of Silane-MXene@MF still exceeds 0.1 MPa and is higher than 90% of the maximum stress of a single compression. It exhibits both exceptional cyclical performance and mechanical stability. Following that, it was studied how the contact angle of Silane-MXene@MF altered after being subjected to acid/alkali treatment by completely soaking it in a solution (HCl/NaCl) with the pH values between 1 and 13 for 24 h. After 24 h, the Silane-MXene@MF was rinsed with ethanol and dried in vacuum drying oven, and then the cleaned foam was observed. As depicted in Figure 9B, after undergoing several acid/alkali treatments, Silane-MXene@MF's contact angle was above 140° while yet retaining a high level of hydrophobicity. Figure 9C depicts the foam's isothermally aged results at 50°C–200°C for 12 h while still maintaining a high hydrophobic angle, highlighting the great heat resistance of Silane-MXene@MF. Because of their outstanding mechanical and hydrophobic durability, the prepared adsorption foams open up the possibility of useful oil-water separation applications in challenging conditions.

4 Conclusion

In the present study, a superhydrophobic and oil-philic Silane-MXene@MF adsorption material was produced by grafting cetyltrimethoxylsilane onto an MXene nano-rough structure on the surface of MF foam. The structure of Silane-MXene@MF was analyzed by infrared and XPS, and the surface morphology was observed by SEM. Silane-MXene@MF has a water contact angle of 157°. It can selectively absorb oil at the water's surface and great depths in the water thanks to its 111 times greater oil absorption capacity than its weight. It works well to separate oil from water in a variety of mixtures. Silane-MXene@MF can also be utilized to efficiently separate oil/water emulsions, and the separation efficiency was as high as 93.12%. After being compressed one hundred times, Silane-MXene@MF still exhibits fantastic cycling performance and mechanical stability, allowing for the recovery of the oil and organics that were adsorbed. Even after being subjected to acid/alkaline treatment for 24 h or isothermal ageing at high temperatures for 12 h, Silane-MXene@MF retains its excellent hydrophobic properties. Due to its simple operation, high stability and stronger oil absorption capacity, Silane-MXene@MF shows considerable promise for use in the treatment of oily wastewater.

Data availability statement

The original contributions presented in the study are included in the article/Supplementary material, further inquiries can be directed to the corresponding author.

Author contributions

WW: Data curation, Writing–review and editing, Writing–original draft. XiS: Validation, Writing–original draft. YX: Methodology, Writing–original draft. XuS: Investigation, Writing–original draft. SZ: Conceptualization, Writing–original draft.

Acknowledgments

The authors would like to acknowledge Qingdao Institute of Bioenergy and Bioprocess Technology for running SEM measurements.

Conflict of interest

Authors WW, XiS, YX, XuS, and SZ were employed by State Key Laboratory of Chemical Safety, SINOPEC Research Institute of Safety Engineering Co, Ltd. The authors declare that this study received funding from SINOPEC. The funder had the following involvement in the study: Preparation and performance testing of functional materials

Publisher's note

References

Beshkar, F., Khojasteh, H., and Salavati-Niasari, M. (2017). Recyclable magnetic superhydrophobic straw soot sponge for highly efficient oil/water separation. *J. Colloid Interface Sci.* 497, 57–65. doi:10.1016/j.jcis.2017.02.016

Chen, C., Zhu, X., and Chen, B. (2019). Durable superhydrophobic/superoleophilic graphene-based foam for high-efficiency oil spill cleanups and recovery. *Environ. Sci. Technol.* 53 (3), 1509–1517. doi:10.1021/acs.est.8b04642

Chen, Y., Wang, N., Guo, F., Hou, L., Liu, J., Liu, J., et al. (2016). A Co_3O_4 nano-needle mesh for highly efficient, high-flux emulsion separation. *J. Mater. Chem. A* 4, 12014–12019. doi:10.1039/c6ta02579j

Dalton, T., and Jin, D. (2010). Extent and frequency of vessel oil spills in US marine protected areas. *Mar. Pollut. Bull.* 60 (11), 1939–1945. doi:10.1016/j.marpolbul.2010.07.036

Doshi, B., Sillanpää, M., and Kalliola, S. (2018). A review of bio-based materials for oil spill treatment. *Water Resarch* 135 (15), 262–277. doi:10.1016/j.watres.2018.02.034

Duan, B., Gao, H., He, M., and Zhang, L. (2014). Hydrophobic modification on surface of chitin sponges for highly effective separation of oil. *ACS Appl. Mater. Interfaces* 6, 19933–19942. doi:10.1021/am505414y

Feng, X., Yu, Z., Long, R., Sun, Y., Wang, M., Li, X., et al. (2020). Polydopamine intimate contacted two-dimensional/two-dimensional ultrathin nylon basement membrane supported RGO/PDA/MXene composite material for oil-water separation and dye removal. *Sep. Purif. Technol.* 247, 116945. doi:10.1016/j.seppur.2020.116945

Gogotsi, Y., and Anasori, B. (2019). The rise of MXenes. *ACS Nano* 13 (8), 8491–8494. doi:10.1021/acsnano.9b06394

Jayaramulu, K., Datta, K. K. R., Rösler, C., Petr, M., Otyepka, M., Zboril, R., et al. (2016). Biomimetic superhydrophobic/superoleophilic highly fluorinated graphene oxide and ZIF-8 composites for oil-water separation. *Angew. Chem. Int. Ed.* 55 (3), 1178–1182. doi:10.1002/anie.201507692

Krasian, T., Punyodom, W., and Worajittiphon, P. (2019). A hybrid of 2D materials (MoS_2 and WS_2) as an effective performance enhancer for poly(lactic acid) fibrous mats in oil adsorption and oil/water separation. *Chem. Eng. J.* 369, 563–575. doi:10.1016/j.cej.2019.03.092

Li, J., Chen, Y., Gao, J., Zuo, Z., Li, Y., Liu, H., et al. (2018). Graphdiyne sponge for direct collection of oils from water. *ACS Appl. Mater. Interfaces* 11 (3), 2591–2598. doi:10.1021/acsami.8b01207

Lin, Z., Shao, H., Xu, K., Taberna, P. L., and Simon, P. (2020). MXenes as high-rate electrodes for energy storage. *Trends Chem.* 2 (7), 654–664. doi:10.1016/j.trechm.2020.04.010

Liu, J., Zhang, H., Sun, R., Liu, Y., Liu, Z., Zhou, A., et al. (2017). Hydrophobic, flexible, and lightweight Mxene foams for high-performance electromagnetic-interference shielding. *Adv. Mater.* 29 (38), 1702367. doi:10.1002/adma.201702367

Liu, L., and Yuan, W. (2018). A hierarchical functionalized biodegradable PLA electrospun nanofibrous membrane with superhydrophobicity and antibacterial properties for oil/water separation. *New J. Chem.* 42, 17615–17624. doi:10.1039/c8nj03112f

Lv, W., Mei, Q., Xiao, J., Du, M., and Zheng, Q. (2017). 3D multiscale superhydrophilic sponges with delicately designed pore size for ultrafast oil/water separation. *Adv. Funct. Mater.* 27 (48), 1704293. doi:10.1002/adfm.201704293

Naguib, M., Kurtoglu, M., Presser, V., Lu, J., Niu, J., Heon, M., et al. (2011). Two-dimensional nanocrystals produced by exfoliation of Ti_3AlC_2. *Adv. Mater.* 23 (37), 4248–4253. doi:10.1002/adma.201102306

Nguyen, D. D., Tai, N., Lee, S., and Kuo, W. (2012). Superhydrophobic and superoleophilic properties of graphene-based sponges fabricated using a facile dip coating method. *Energy & Environ. Sci.* 5, 7908–7912. doi:10.1039/c2ee21848h

Peng, J., Deng, J., Quan, Y., Yu, C., Wang, H., Gong, Y., et al. (2018). Superhydrophobic melamine sponge coated with striped polydimethylsiloxane by thiol-ene click reaction for efficient oil/water separation. *ACS Omega* 3 (5), 5222–5228. doi:10.1021/acsomega.8b00373

Pham, V. H., and Dickerson, J. H. (2014). Superhydrophobic silanized melamine sponges as high efficiency oil absorbent materials. *ACS Appl. Mater. interfaces* 6 (16), 14181–14188. doi:10.1021/am503503m

Qian, X., Fan, X., Peng, Y., Xue, P., Sun, C., Shi, X., et al. (2020). Polysiloxane cross-linked mechanically stable Mxene-based lithium host for ultrastable lithium metal anodes with ultrahigh current densities and capacities. *Adv. Funct. Mater.* 31 (6), 2008044. doi:10.1002/adfm.202008044

Saththasivam, J., Wang, K., Yiming, W., Liu, Z., and Mahmoud, K. A. (2019). A flexible $Ti_3C_2T_x$ (MXene)/paper membrane for efficient oil/water separation. *RSC Adv.* 9, 16296–16304. doi:10.1039/c9ra02129a

Shahzad, F., Alhabeb, M., Hatter, C. B., Anasori, B., Hong, S. M., Koo, C. M., et al. (2016). Electromagnetic interference shielding with 2D transition metal carbides (MXenes). *Science* 353 (6304), 1137–1140. doi:10.1126/science.aag2421

Shannon, M. A., Bohn, P. W., Elimelech, M., Georgiadis, J. G., Mariñas, B. J., and Mayes, A. M. (2008). Science and technology for water purification in the coming decades. *Nature* 452, 301–310. doi:10.1038/nature06599

Song, P., Liu, B., Qiu, H., Shi, X., Cao, D., and Gu, J. (2021). MXenes for polymer matrix electromagnetic interference shielding composites: a review. *Compos. Commun.* 24, 100653. doi:10.1016/j.coco.2021.100653

Wang, C. F., and Lin, S. J. (2013). Robust superhydrophobic/superoleophilic sponge for effective continuous absorption and expulsion of oil pollutants from water. *ACS Appl. Mater. Interfaces* 5 (18), 8861–8864. doi:10.1021/am403266v

Wang, N., Wang, H., Wang, Y., Wei, Y., Si, J., Yuen, A. C. Y., et al. (2019). Robust, lightweight, hydrophobic, and fire-retarded polyimide/MXene aerogels for effective oil/water separation. *ACS Appl. Mater. Interfaces* 11 (43), 40512–40523. doi:10.1021/acsami.9b14265

Wu, Z., Feng, X., Qu, Y., Gong, L., Cao, K., Zhang, G., et al. (2023). Silane modified MXene/polybenzazole nanocomposite aerogels with exceptional surface hydrophobicity, flame retardance and thermal insulation. *Compos. Commun.* 37, 101402. doi:10.1016/j.coco.2022.101402

Xia, C., Li, Y., Fei, T., and Gong, W. (2018). Facile one-pot synthesis of superhydrophobic reduced graphene oxide-coated polyurethane sponge at the

presence of ethanol for oil-water separation. *Chem. Eng. J.* 345, 648–658. doi:10.1016/j.cej.2018.01.079

Xu, M., Futaba, D. N., Yamada, T., Yumura, M., and Hata, K. (2010). Carbon nanotubes with temperature-invariant viscoelasticity from -196° to 1000 °C. *Science* 330 (6009), 1364–1368. doi:10.1126/science.1194865

Xue, J., Zhu, L., Zhu, X., Li, H., Ma, C., Yu, S., et al. (2021). Tetradecylamine-MXene functionalized melamine sponge for effective oil/water separation and selective oil adsorption. *Sep. Purif. Technol.* 259, 118106. doi:10.1016/j.seppur.2020.118106

Yan, J., Ren, C. E., Maleski, K., Hatter, C. B., Anasori, B., Urbankowski, P., et al. (2017). Flexible MXene/graphene films for ultrafast supercapacitors with outstanding volumetric capacitance. *Adv. Funct. Mater.* 27 (30), 1701264. doi:10.1002/adfm.201701264

Yang, Y., Deng, Y., Tong, Z., and Wang, C. (2014). Multifunctional foams derived from poly(melamine formaldehyde) as recyclable oil absorbents. *J. Mater. Chem. A* 2, 9994–9999. doi:10.1039/c4ta00939h

Zhang, D., Lin, Y., Wang, W., Li, Y., and Wu, G. (2021). Mechanically strong polyimide aerogels cross-linked with dopamine-functionalized carbon nanotubes for oil absorption. *Appl. Surf. Sci.* 543 (30), 148833. doi:10.1016/j.apsusc.2020.148833

Zhang, J., Li, B., Li, L., and Wang, A. (2016a). Ultralight, compressible and multifunctional carbon aerogels based on natural tubular cellulose. *J. Mater. Chem. A* 4, 2069–2074. doi:10.1039/c5ta10001a

Zhang, W., Zhai, X., Xiang, T., Zhou, M., Zang, D., Gao, Z., et al. (2016b). Superhydrophobic melamine sponge with excellent surface selectivity and fire retardancy for oil absorption. *J. Mater. Sci.* 52, 73–85. doi:10.1007/s10853-016-0235-7

Zhao, S., Zhang, H., Luo, J., Wang, Q., Xu, B., Hong, S., et al. (2018). Highly electrically conductive three-dimensional $Ti_3C_2T_x$ MXene/reduced graphene oxide hybrid aerogels with excellent electromagnetic interference shielding performances. *ACS Nano* 12 (11), 11193–11202. doi:10.1021/acsnano.8b05739

Zhu, H., Chen, D., An, W., Li, N., Xu, Q., Li, H., et al. (2015). A robust and cost-effective superhydrophobic graphene foam for efficient oil and organic solvent recovery. *Small* 11 (39), 5222–5229. doi:10.1002/smll.201501004